

T. BOROWSKI<sup>1\*</sup>, K. KULIKOWSKI<sup>1</sup>, M. SPYCHALSKI<sup>1</sup>, K. ROŻNIATOWSKI<sup>1</sup>,  
B. RAJCHEL<sup>2</sup>, B. ADAMCZYK-CIEŚLAK<sup>1</sup>, T. WIERZCHOŃ<sup>1</sup>

## MECHANICAL BEHAVIOR OF NITROCARBURISED AUSTENITIC STEEL COATED WITH N-DLC BY MEANS OF DC AND PULSED GLOW DISCHARGE

AISI 316L steel was subjected to nitrocarburizing under glow discharge conditions, which was followed by DLC (diamond-like carbon) coatings deposition using the same device. The coatings were applied under conditions of direct current and pulsed glow discharge. In order to determine the influence of the produced nitrocarbon austenite layer and the type of discharge on the microstructure and mechanical properties of the coatings, the following features were analysed: surface roughness, coating thickness, structure, chemical composition, adhesion and resistance to frictional wear. For comparison purposes, DLC coatings were also deposited on steel without a nitrocarburised layer. The obtained results indicate a significant influence of the type of glow discharge on the roughness, hardness, nitrogen content and of the nitrocarburised layer on the resistance to wear by friction and adhesion of the produced coatings.

*Keywords:* DLC; nitrocarburizing; surface engineering; hardness; adhesion; wear

### 1. Introduction

Diamond-like carbon (DLC) is a generic term used to describe a wide range of amorphous carbon coatings. These include, among others, amorphous carbon (a-C) and hydrogenated amorphous carbon (a-C:H) [1]. Coatings of the a-C:H type are mainly produced using CVD methods with hydrocarbon gases such as methane or acetylene, whereas a-C coatings are mainly deposited using PVD methods, where graphite is used as the sputtering target [2]. Carbon occurs in many forms, of which the two most common include diamond (in  $sp^3$  hybridization) and graphite (in  $sp^2$  hybridization) [3]. In turn, the structure of a DLC coating comprises a mixture of  $sp^3$  and  $sp^2$  hybridization bonds, whose mutual ratio determines the coating's mechanical properties [4,5]. DLC coatings have been widely studied in recent years due to their low friction coefficient, resistance to wear, high hardness, biocompatibility and chemical inertness [6]. The combination of these properties has made the coatings popular in various industries, e.g. automotive, medical, military and paper. DLC coatings are often enriched with various elements, such as Si [7-10], Ti [11], F [12], W [13], Cr [14], N [15-17] in order to alter stress, surface energy

or modify their adhesion to the substrate, their hardness, wear resistance or thermal stability. The introduction of nitrogen into the structure of a DLC coating is one of the main methods of reducing its residual stress levels, an alteration that lowers the hardness of the coating but also improves its adhesion to the substrate [18]. Nitrogen is capable of breaking  $sp^3$  bonds and, consequently, changing a part of the structure into graphite ( $sp^2$  bonds), resulting in a reduction of frictional forces and wear [18,19]. DLC coatings usually demonstrate poor adhesion to soft substrates [20]. The thermal expansion coefficients of the coating and substrate are often different, which results in the coating's high stress values and weak adhesion [21]. In order to eliminate this problem, attempts have been made to apply different interlayers [22-26]. Nitrocarburizing is one of many thermo-chemical treatments that makes it possible to increase the surface hardness of steel. Unlike with austenitic steel nitriding, nitrocarburizing yields thicker layers with a higher gradient [27]. During low-temperature nitrocarburizing of austenitic steel ( $<450^\circ\text{C}$ ), an S-phase (nitrocarbon expanded austenite) is formed in the surface layer [27-28]. Several publications deal with the deposition of DLC coatings on the nitrocarburised layer and concern mainly research on AISI H13 [29-31],

<sup>1</sup> WARSAW UNIVERSITY OF TECHNOLOGY, FACULTY OF MATERIALS SCIENCE AND ENGINEERING, 141 WOŁOSKA STR., 02-507 WARSZAWA, POLAND

<sup>2</sup> POLISH ACADEMY OF SCIENCES, INSTITUTE OF NUCLEAR PHYSICS, POLAND

\* Corresponding author: [austenmart@gmail.com](mailto:austenmart@gmail.com)



4140 [32], 410 [33] and 304 [34] steels. Therefore, it can be concluded that few studies have been carried out in recent years on DLC coatings formed on nitrocarbon layers, in particular on the nitrocarbon S-phase layer produced on commonly used AISI 316L steel [35]. It is also difficult to find studies dealing with the influence of the glow discharge type (direct current and pulsed) on the properties of deposited coatings. For these reasons, the aim of the study was to investigate the influence of DC and pulsed glow discharge processes used in the application of N-DLC coatings, and the influence of nitrocarbon austenite layers produced on austenitic 316L steel, on the structure, roughness, adhesion, wear resistance and friction coefficient of the coatings. Another novelty introduced by the study is the possibility to produce a hardened diffusion layer and a carbon-based coating using one device for conducting glow discharge processes.

## 2. Materials and methods

The test specimens were cut from a round rod of AISI 316L steel with the following chemical composition in wt %: C < 0.03, Si < 0.08, Mn < 2, P < 0.045, S < 0.03, Cr 16-18, Mo 2-2.5, Ni 12-15, the rest being Fe. The samples were  $\phi 25 \times 4$  mm in size and their flat surfaces were ground using 240 to 800-grit SiC sandpaper. The prepared samples were degreased in acetone in an ultrasonic cleaner and then washed in distilled water. Half of the samples were first plasma nitrocarburised at 440°C for 6 hours, at a working chamber pressure of 100 Pa, while the working mixture composition was as follows: N<sub>2</sub> and H<sub>2</sub> at a ratio of 1:3, and CH<sub>4</sub>, which made up 5% of the entire gas mixture. A voltage of 898 V and a current of 1.3 A were applied. Next, carbon-based coatings were deposited on steel in initial state (IS) and on a nitrocarburised layer (NC). DLC coatings were produced under direct current glow discharge conditions for 20 minutes at 350°C, in a CH<sub>4</sub>:N<sub>2</sub> atmosphere, at a working gas ratio of 9:1, working chamber pressure of 450 Pa, an applied current of 0.34 A and a voltage of 400 V. The pulsed discharge process employed a current of 0.44 A at 840 V and 160 kHz frequency. Four variants of DLC coatings were studied, i.e. produced under DC discharge on steel in initial state without a layer (IS-DLC-DC) and with a nitrocarbon layer (NC-DLC-DC), and produced under pulsed discharge on steel without a layer (IS-DLC-P) and with a diffusion layer (NC-DLC-P). The surface roughness parameters (Ra, Rq, Rz) of 316L steel, the nitrocarburised layer and the DLC coatings were measured using a Veeco atomic force microscope with a Multimode V controller (tapping mode, tip model ACSTA, AppNano). A Raman spectrometer (ALMEGA XR by Thermo) excited with a 532 nm laser, at an operating power of 25 mW was employed to characterise the deposited DLC coatings. To verify any changes in the local bonding structure, the I<sub>D</sub>/I<sub>G</sub> ratio was calculated from the fitted D and G peaks. The coating's nitrogen content was measured using Thermo Noran's energy dispersive spectrometer. The application of an accelerating voltage with a value of 10 kV made it possible to eliminate the influence of

the nitrogen present in the nitrocarburised layer and of other elements occurring in the substrate. The surfaces of the samples prepared for thickness and microstructure analysis were ground along the layers' cross-sections using SiC abrasive papers up to #1200 grit and then polished with a 1 mm diamond suspension and etched using a reagent with the following composition: 50% HCl + 25% HNO<sub>3</sub> + 25% H<sub>2</sub>O. Afterwards, the coatings and layers were analyzed along the samples' cross-sections using a Nikon Eclipse LV150N optical microscope. X-ray diffraction analysis of the NC layer and of the IS specimen was carried out using a Bruker D8 Advance X-ray diffractometer via CuK<sub>α</sub> filtered radiation ( $\lambda = 0.154056$  nm) at room temperature. The recording conditions were as follows: voltage 40 kV, current 40 mA, 2 $\theta$  angular range from 25° to 65°, step D2Q – 0.05°, count time – 3 s. The recorded diffraction patterns were analysed using Bruker's EVA software. The microhardness of 316L steel and of the nitrocarbon layer was measured on their surfaces under a 50 g load (HV0.05) using a ZWICK microhardness tester. Nanoindentation tests of the DLC coatings were conducted on a Hysitron Ti 950 TriboIndenter. A trapezoid course of the load was used for the tests and the device was operated in force feedback-control mode. A maximum load of 10 mN was used. The load of the indenter was set to a value preventing it from exceeding a depth of 1/5 of the coating thickness, which was essential to eliminate the elastic effect of the substrate. The measurements were based on the hardness of the coatings and reduced Young's modulus. Adhesion testing of the layers was carried out on a CSM scratch-test device using a Rockwell diamond indenter with a tip radius of 0.8 mm. The test sample was moved at a constant speed perpendicular to the tip. The scratch lengths for all the measurements were 5 mm and the contact force varied linearly from 1 to 20 N. Analysis of the coatings' adhesion was based on scratch observations using a Nikon LV150N Eclipse microscope. "Ball-on-disc" frictional wear tests were performed on a T-21 tribotester manufactured by ITEE Radom in accordance with ASTM G 99-05, ISO 20808:2004. Al<sub>2</sub>O<sub>3</sub>, 10 mm diameter ceramic balls with a polished surface were used. The tests were carried out at a load of 5 N, a slip speed of 0.105 m/s, whereas measurements were made over the course of 5000 revolutions. Wear resistance was determined on the basis of measuring the size of groove profile (wear). Groove geometry was measured with the use of the Veeco optical profilometer while its cross section area was calculated by computer program Vision<sup>R</sup>. Wear rate was determined according to the following equation:

$$W_v = \frac{V}{F_n \cdot s} \left[ \frac{\text{mm}^3}{\text{N} \cdot \text{m}} \right] \quad (1)$$

where:  $V$  – worn material volume calculated on the basis of the average size of groove's cross section area,  $F_n$  – axial force,  $s$  – friction track length.

The wear indexes and changes in the friction coefficient were presented on graphs and a WYKO NT9300 optical profilometer was used to illustrate the wear tracks.

### 3. Results and discussion

The temperature of 440°C made it possible to create a layer of nitrocarbon expanded austenite (S-phase), which was free from iron and chromium carbonitrides, as evidenced by XRD examinations and shown in Fig. 1. In the case of initial state steel (IS), a peak from the deformation-induced martensite that formed as a result of pressure applied during surface grinding (TRIP effect), was visible alongside the austenite peaks. Nitrocarburizing led to the reverse transformation of martensite to austenite. As a result of this process, martensite was no longer observed in the diffusion layer. A decrease of the austenitic transformation start temperature ( $A_s$ ) takes place as the concentration of nitrogen and carbon in the structure increases. At a certain concentration of these elements, the  $A_s$  temperature reaches a value equal to the process temperature (440°C) resulting in the transformation of nitrocarbon martensite to reversed nitrocarbon S-phase. This phenomenon has already been observed by other researchers in nitrated 304 austenitic steel previously subjected to martensitic transformations [36]. The layer presents a hardness of  $972 \pm 8$  HV0.05, while the hardness of the core amounted to  $264 \pm 3$  HV0.05.

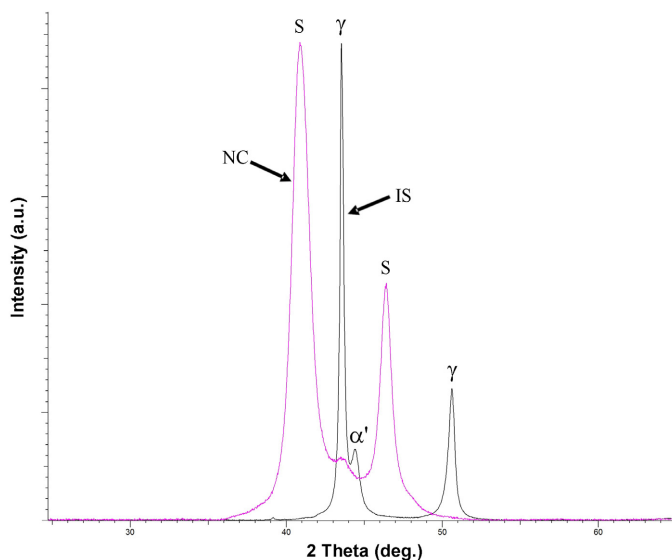


Fig. 1. XRD patterns for 316L steel in initial state (IS) and after NC process

Table 1 shows the roughness parameters of the 316L steel surface in initial state (IS), after nitrocarburizing (NC) and with coatings produced under DC (IS-DLC-DC, NC-DLC-DC) and pulsed (IS-DLC-P, NC-DLC-P) glow discharge conditions. The roughness of the steel surface changed after nitrocarburizing, which is reflected in the Ra, Rq and Rz parameters, which increased, e.g. from Ra = 33.4 nm to Ra = 40.5 nm (Tab. 1). The deposition of DLC coatings under DC glow discharge conditions on the surface of steel without a layer and with a layer of nitrocarbon austenite resulted in a significant increase in roughness. The coating produced on steel in the initial state (IS-DLC-DC) was characterised by almost double the roughness value, while

the coating applied on the layer (NC-DLC-DC) was more than twice as rough as the NC layer, taking into account the Ra and Rq parameters. On the other hand, the application of pulsed glow discharge produced a different effect. A smoothing of the coatings' surface was observed, i.e. for the coating on steel in initial state (IS-DLC-P), the Ra, Rq parameters decreased by half in comparison to steel without any layers (IS), while for the coating applied onto a layer of nitrocarbon austenite (NC-DLC-P) the roughness parameters Ra, Rq and Rz was slightly higher than the roughness of the diffusion layer's surface without a coating (NC). It can be stated that the choice of glow discharge type has a significant influence on the surface quality of DLC coatings, which is particularly important when considering the material for use in elements intended to operate in conditions of friction.

TABLE 1

Surface roughness (Ra, Rq, Rz) of steel in initial state (IS), steel with coatings: IS-DLC-DC, IS-DLC-P, of NC layer and NC layer with coatings: NC-DLC-DC, NC-DLC-P measured with an AFM

Material	Ra [nm]	Rq [nm]	Rz [nm]
IS	33.4 ± 1.2	42.8 ± 1.4	285 ± 12
IS-DLC-DC	58.4 ± 3.5	74 ± 4.7	517 ± 18
IS-DLC-P	15.2 ± 0.7	19.3 ± 0.9	198 ± 9
NC	40.5 ± 2.3	53 ± 2.9	776 ± 24
NC-DLC-DC	82.3 ± 5.2	105 ± 7.8	801 ± 32
NC-DLC-P	43.9 ± 2.6	55.4 ± 3.1	785 ± 27

As shown in Table 2, coatings applied under DC discharge showed the highest nitrogen content, which exceeded 14% at. A slightly higher concentration of this element was observed in the IS-DLC-DC coating compared to NC-DLC-DC. Under pulsed discharge conditions the nitrogen content was the lowest and amounted to about 10% at., with the IS-DLC-P coating showing a slightly higher nitrogen content. Differences in the concentrations of this element in the coatings also affected the  $I_D/I_G$  ratio. It is emphasised that the higher the nitrogen content in the coating, the higher the  $I_D/I_G$  value, which proves the existence of a structure with a higher share of  $sp^2$  graphite bonds [18,31]. Introduction of nitrogen into the structure of the carbon layer causes that hydrogen atoms to be replaced by nitrogen atoms, which reduces the number of C-H bonds and accelerates the transformation of  $sp^3$  into  $sp^2$ . This results from the fact that C-H bonds in the coating play a key role in the stabilization of  $sp^3$  diamond bonds [37]. The lowest  $I_D/I_G$  value was observed for DLC coatings produced in pulsed discharge conditions, i.e. where the lowest nitrogen content was detected ( $I_D/I_G = 0.54$  for IS-DLC-P and 0.53 for NC-DLC-P coating). Figure 2 shows cross-sectional micrographs of coatings produced under DC (Fig. 2a) and pulsed (Fig. 2b) glow discharge conditions on the nitrocarbon S-phase layer of 316L austenitic steel substrate. The nitrocarburised layer produced on austenitic steel at 440°C presents a dual-layer structure comprising two separated layers consisting of an outer nitrocarbon S-phase and an inner, thinner carbon S-phase with a total thickness of about 10.5  $\mu\text{m}$ . This characteristic structure of the nitrocarburised layer results from the differences in the

diffusion coefficients of carbon and nitrogen within austenite [28,38,39]. It can be observed that the produced DLC coatings are homogeneous and of uniform thickness. The coatings differ in thickness depending on the type of glow-discharge applied.

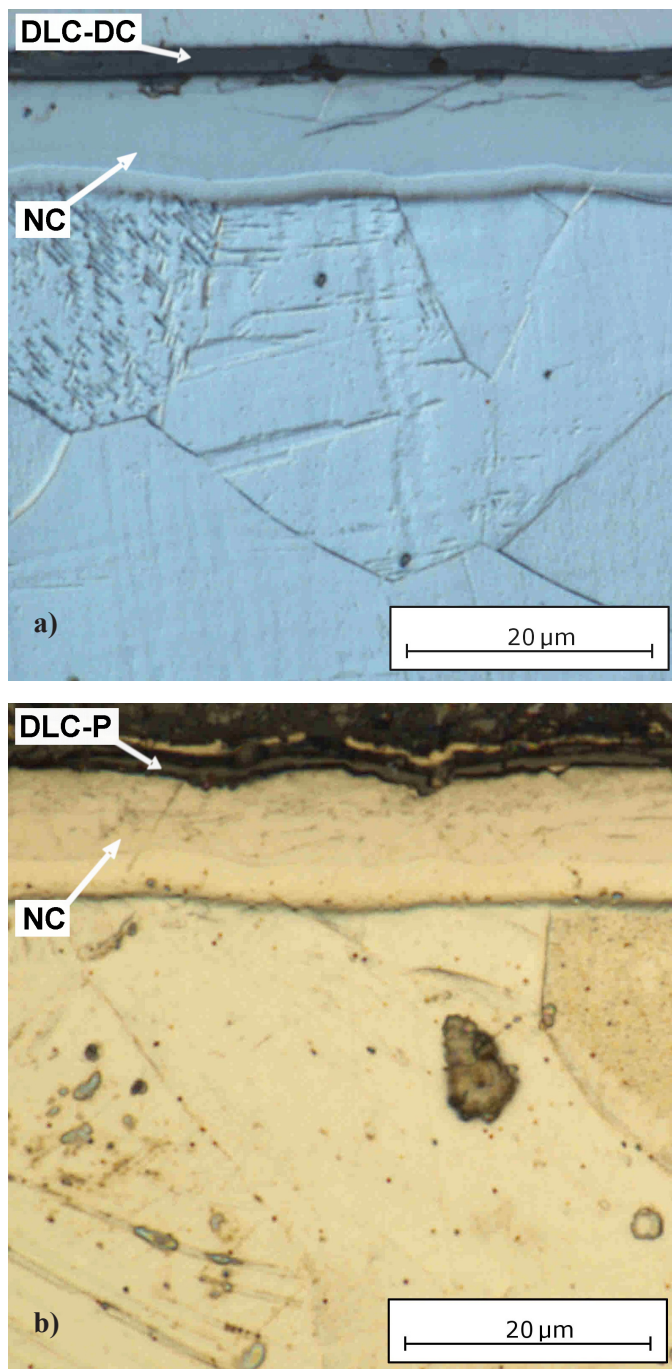


Fig. 2. Cross-section images of a) NC-DLC-DC and b) NC-DLC-P layers

For DC discharge, the coatings had a thickness of about 2 µm (Fig. 2a, Tab. 2), with NC-DLC-DC producing slightly thicker coatings (2.14 µm). For pulsed discharge, the thickness of the IS-DLC-P and NC-DLC-P coatings was very similar and amounted to approximately 0.85 µm (Fig. 2b, Tab. 2). Significant differences in the thickness of coatings produced under DC and pulsed discharge conditions may result from variations in the

voltages applied during coating deposition. In order to maintain the desired temperature during pulsed discharge, the voltage was approximately 440 V higher than in the DC discharge process. Under these conditions, cathodic sputtering may occur more intensively alongside coating deposition, resulting in a thinner coating.

TABLE 2

Nitrogen content (N),  $I_D/I_G$  ratio and thickness (d) of IS-DLC-DC, IS-DLC-P, NC-DLC-DC, NC-DLC-P coatings

Material	N [at %]	$I_D/I_G$	d [µm]
IS-DLC-DC	14.6 ± 1.9	0.71	2.00 ± 0.03
IS-DLC-P	10.2 ± 1.3	0.54	0.85 ± 0.02
NC-DLC-DC	14.2 ± 2.0	0.83	2.14 ± 0.03
NC-DLC-P	9.9 ± 1.3	0.53	0.86 ± 0.03

Values of hardness and reduced Young's modulus of elasticity for coatings produced under direct current glow discharge conditions were similar and amounted to 3.4 GPa and 34.9 GPa for the IS-DLC-DC coating and 3.5 GPa and 35.1 GPa for the NC-DLC-DC coating respectively, as shown in Table 3. A similar situation can be observed for coatings produced under pulsed glow discharge conditions. In this case, the IS-DLC-P coating had a hardness of 12.3 GPa and the reduced modulus was 126 GPa, while for the NC-DLC-P coating the values were 12.5 GPa and 129 GPa, respectively. A slight increase in the hardness of NC-DLC-DC and NC-DLC-P coatings compared to IS-DLC-DC and IS-DLC-P coatings (0.1 GPa for DC discharge and 0.2 GPa for pulsed discharge) probably results from the lower nitrogen content in the coatings produced on the nitrocarbon layers (Tab. 2). As already noted, the nitrogen introduced into the structure of the coating facilitates the transformation of  $sp^3$  into  $sp^2$ , which results in a change of hardness [18]. Using pulsed discharge instead of DC discharge resulted in the formation of coatings with a 60% lower thickness and lower nitrogen content, which in turn resulted in a lower share of the graphite structure (Tab. 2) and, consequently, in a nearly four times greater hardness value (Tab. 3). Ruijun et al. [16] produced DLC coatings with a nitrogen concentration of 4.1 to 7.8% at. on silicon by using the ECWR-CVD method. They managed to achieve a hardness of 9.07 GPa and a reduced Young's modulus of 65.43 GPa for a nitrogen content of 4.1% at. and 0.874 GPa and 1.68 GPa respectively for a content of 7.8% at. In turn, Sharifahmadian [29] recorded a hardness of 13.83 GPa in a DLC coating containing 19% at. nitrogen produced by means of the DC PACVD method on nitrocarburised H13 steel. It can therefore be concluded that the hardness and reduced Young's modulus values obtained in this study (Tab. 3) at a relatively high nitrogen content in the coatings (Tab. 2) are similar to those achieved by other scientists.

The results of nitrogen content and hardness were also reflected in tests carried out to verify adhesion of the coatings to the substrate by means of the scratch-test method (Fig. 3). Coatings deposited on steel in initial state underwent mainly plastic deformation under the action of an indenter. For the IS-DLC-DC coating, the main cause of the deformation was

TABLE 3

Hardness (H) and reduced Young's modulus (Er) of IS-DLC-DC, IS-DLC-P, NC-DLC-DC, NC-DLC-P coatings

Material	H [GPa]	Er [GPa]
IS-DLC-DC	3.4 ± 0.2	34.9 ± 1.3
IS-DLC-P	12.3 ± 0.4	126 ± 3.1
NC-DLC-DC	3.5 ± 0.2	35.1 ± 1.1
NC-DLC-P	12.5 ± 0.5	129 ± 3.4

a low hardness value due to a significant nitrogen content in the coating (over 14% at.) (Fig. 3a), however, no delamination was observed. For the IS-DLC-P coating, on the other hand, the deformation resulted from its lower thickness (0.85 μm) and the interaction of the soft substrate (Fig. 3b). In this coating, the first chipping was also observed at a load of 5.4 N, but during the subsequent load increase up to 20 N, the coating did not delaminate. No plastic deformations were observed in coatings formed on the NC layer, which confirms the positive influence of a hard substrate with a layer made of the S-phase (Fig. 3c,d). For NC-DLC-DC coatings, practically no surface changes were observed. Two minor chips were observed on the NC-DLC-P coating, the first of them appearing at a load of 6.5 N. The nitrocarburised layer plays a significant role in the transfer of loads applied to the surface of the coatings by minimizing their deformation. In turn, the deformations observed on the surfaces of the coatings produced on un-pretreated steel (IS-DLC-DC, IS-DLC-P) are caused by the soft substrate undergoing plastic deformation together with the coating as it interacts with the indenter. The reason for the superior adhesion of NC-DLC-DC and NC-DLC-P coatings may also be the presence of carbon in the diffusion layer which increases the affinity of the coating to the nitrocarbon layer.

“Ball-on-disc” tests at a load of 5 N have proved that all the applied surface treatment methods reduce the friction coefficient and improve the wear resistance of 316L steel, as

shown in Fig. 4, 5. Initial steel showed a significant degree of frictional wear (Fig. 6a) amounting to  $429 \cdot 10^{-9} \text{ mm}^3/\text{N}\cdot\text{m}$ . Steel with the NC layer showed a lower coefficient of friction (ca. 0.6) compared to steel in its initial state (ca. 0.7) (Fig. 4), as well as lower wear, which decreased to  $8.72 \cdot 10^{-9} \text{ mm}^3/\text{N}\cdot\text{m}$  (Fig. 5). The presence of carbon in the S-phase is the main cause of the reduction in friction force, which results in a lower coefficient of friction. This observation has been reported in other studies as well [38,40]. The deposition of DLC coatings caused an additional decrease in the friction coefficient and a significant decrease in the degree of wear rates (Fig. 4, 5). The IS-DLC-P coating showed the lowest coefficient of friction (ca. 0.14), which resulted mainly from its high smoothness (Tab. 1) and increased hardness (Tab. 3), these two factors also contributing to the lowest wear rate ( $0.39 \cdot 10^{-9} \text{ mm}^3/\text{N}\cdot\text{m}$ ). It is observed that the very low roughness and relatively high hardness of the coating are sufficient to ensure resistance to frictional wear in the proposed test conditions despite the lack of a hardened surface. The NC-DLC-DC coating showed a similarly low coefficient of friction (ca. 0.15) and an almost equally low wear rate ( $0.79 \cdot 10^{-9} \text{ mm}^3/\text{N}\cdot\text{m}$ ), which may be the result of a higher content of the graphite phase caused by the introduction of a greater amount of nitrogen into the coating structure. The friction course for both the above coatings was stable (Fig. 4). The NC-DLC-P coating was harder (12.5 GPa), however, due to its smaller thickness (0.86 μm) and a roughness that was slightly higher than that of the NC layer, its friction coefficient remained at ca. 0.24 (Fig. 4), while the wear rate at  $1.82 \cdot 10^{-9} \text{ mm}^3/\text{N}\cdot\text{m}$  (Fig. 5). The IS-DLC-DC coating demonstrated the highest coefficient of friction (ca. 0.32) and wear rate ( $9.32 \cdot 10^{-9} \text{ mm}^3/\text{N}\cdot\text{m}$ ) from among all the coatings. The course of friction for this coating was not stable and the frictional force increased as the test continued (Fig. 4). A higher content of graphite bonds in this coating and its significant thickness (Tab. 2) should have guaranteed lower coefficients of friction

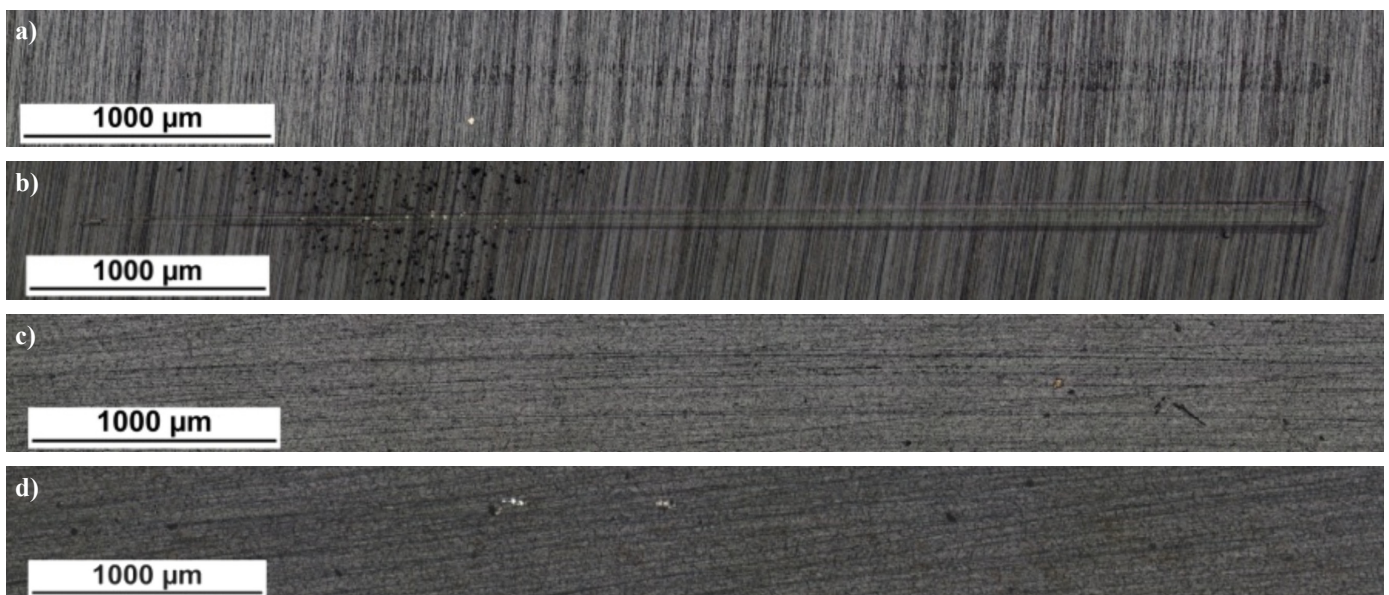


Fig. 3. Scratch-test images of a) IS-DLC-DC, b) IS-DLC-P, c) NC-DLC-DC, d) NC-DLC-P coatings

and wear. However, the main reason for the increase in these parameters was the coating's low hardness value and the fact that the substrate it was applied on was not hardened. The increase was also partly caused by the surface roughness of the coating, which was almost twice as high as the roughness of steel in initial state (Tab. 1). As a result of the lower hardness of the coating and the substrate, the contact surface of the sample with the counter-sample increased during friction, which in turn altered the interaction between the two and significantly increased friction. The selected test conditions (5N load and countersample geometry) did not cause delamination or decohesion of the produced coatings, and therefore no typical forms of wear, such as chipping and cracking of the coatings, were observed. The main type of wear consisted of plastic deformation and frictional wear of the coatings' surfaces (Fig. 6b). In the case of coatings produced on the nitrocarburised layer (NC-DLC-DC and NC-DLC-P) there was a clear decrease in wear rates (Fig. 5) resulting mainly from the interaction of the hardened steel substrate. During the tests, the hard nitrocarburised layer prevented any significant deformation of the coatings, thanks to which the contact surface of the ceramic counter-sample with the surface of the coatings was relatively small resulting in low frictional

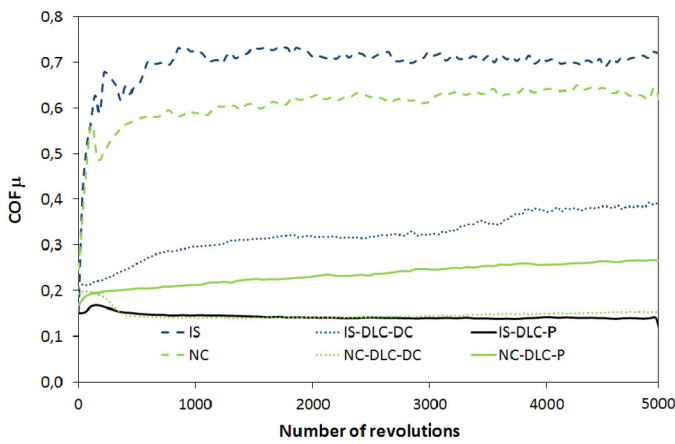


Fig. 4. Course of the friction coefficient during the “ball-on-disc” test at 5 N for steel in initial state (IS), steel with coatings: IS-DLC-DC, IS-DLC-P, for NC layer and NC layer with coatings: NC-DLC-DC, NC-DLC-P

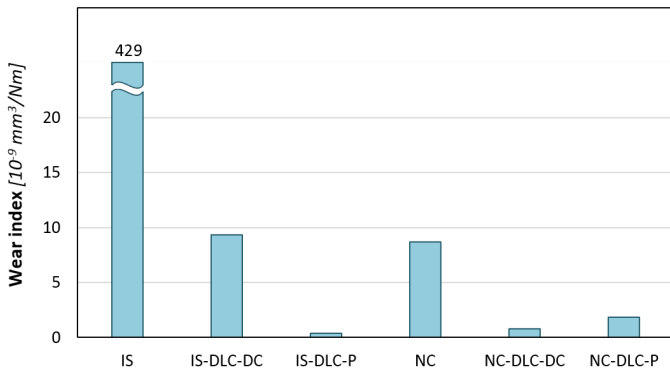


Fig. 5. Wear indexes obtained in “ball-on-disc” tests at a load of 5 N for steel in initial state (IS), steel with coatings: IS-DLC-DC, IS-DLC-P, for NC layer and NC layer with coatings: NC-DLC-DC, NC-DLC-P

forces and wear rates. Sharifahmadian et al. [29] applied DLC coatings onto H13 nitrocarbon steel using the PACVD method. The coefficients of friction for DLC coatings with a nitrogen content of 10-15% at. were similar to those presented in this paper and ranged from 0.2 to 0.3. The wear rates were higher ( $1,15 \cdot 10^{-6}$ - $1,82 \cdot 10^{-6}$  mm<sup>3</sup>/N·m), however, the authors of the paper used a 5 mm diameter SiC ceramic ball, which had a significant impact on the contact geometry in the friction node and, due to the reduced contact surface, increased the value of stress between the sample and the counter-sample. It is concluded that nitrogen-doped DLC coatings deposited on 316L nitrocarburised steel under DC and pulsed glow discharge conditions present promising results in terms of frictional wear resistance, but require further analysis and testing at higher loads.

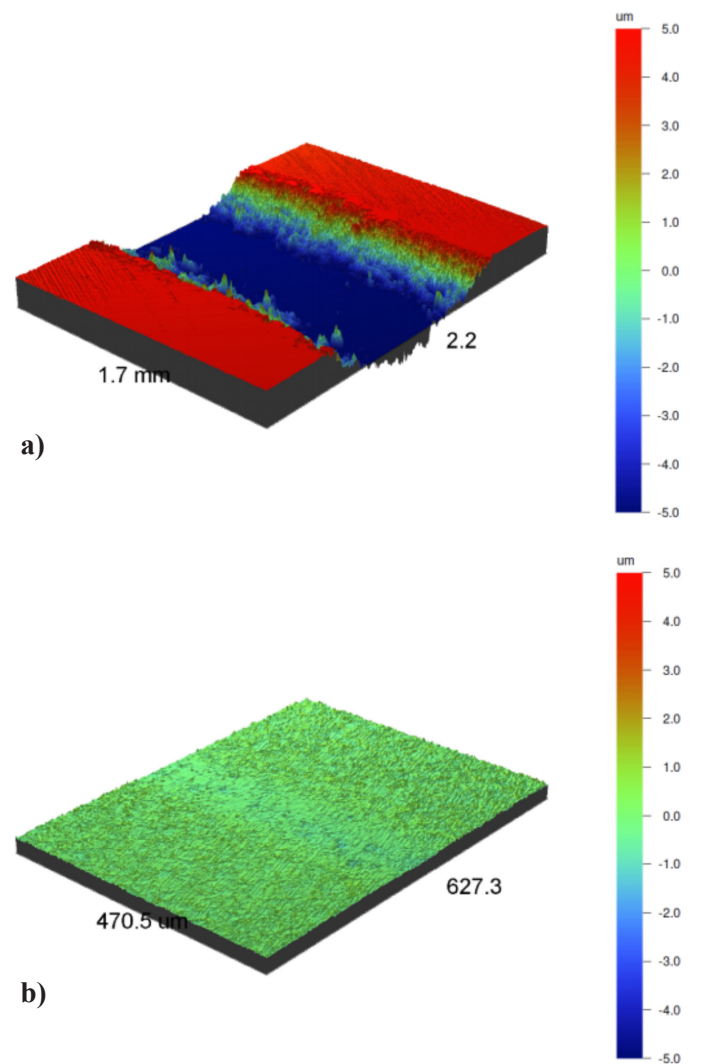


Fig. 6. A selected 3D images of wear tracks obtained in “ball-on-disc” tests at 5 N for a) steel in initial state (IS) and for b) NC-DLC-P coating

#### 4. Conclusions

- Based on the results obtained, it can be concluded that:
- The application of DC glow discharge results in coatings with a higher nitrogen content and a higher  $I_D/I_G$  ratio,

which confirms the presence of a higher number of  $sp^2$  bonds. These in turn lead to a decrease in hardness but also improve adhesion to the substrate, which is particularly noticeable for coating deposition on the nitrocarbon layer.

- Deposition of DLC coatings on 316L steel and on a layer of nitrocarbon austenite results in a reduction of the friction coefficient and wear rates as shown in the “ball-on-disc” tests.
- The best adhesion and low wear rates are observed in coatings produced on the nitrocarbon austenite layer.
- The DLC coating produced under pulsed glow discharge conditions on 316L steel without a layer showed the lowest coefficient of friction and wear due to the relatively high hardness and the lowest roughness of the surface. However, due to the lower thickness of the DLC coating and the unhardened substrate, the coating underwent plastic deformation during the scratch-test.

#### Acknowledgments

This work was supported by The National Science Centre [grant No. 2012/07/D/ST8/02599].

#### REFERENCES

- [1] J. Robertson, *Mater. Sci. and Eng.* **R 37**, 129-281 (2002). DOI: [https://doi.org/10.1016/S0927-796X\(02\)00005-0](https://doi.org/10.1016/S0927-796X(02)00005-0)
- [2] H. Moriguchi, H. Ohara, M. Tsujioka, *Sei Technical Review* **82**, 52-58 (2016).
- [3] Bewilogua, D. Hofmann, *Surf. and Coat. Technol.* **242**, 214-225 (2014). DOI: <https://doi.org/10.1016/j.surfcoat.2014.01.031>
- [4] G. Capote, L.F. Bonetti, L.V. Santos, V.J. Trava-Airoldi, E.J. Corat, *Thin Solid Films* **516**, 4011-4017 (2008). DOI: <https://doi.org/10.1016/j.tsf.2007.08.007>
- [5] Gupta, V. Singh, E.I. Meletis, *Tribol. Int.* **37**, 1019-1029 (2004). DOI: <https://doi.org/10.1016/j.triboint.2004.07.020>
- [6] A. Grill, Diamond-like carbon: state of the art, *Diam. & Relat. Mater.* **8**, 428-434 (1999). DOI: [https://doi.org/10.1016/S0925-9635\(98\)00262-3](https://doi.org/10.1016/S0925-9635(98)00262-3)
- [7] S.C. Ray, D. Mukherjee, S. Sarma, G. Bhattacharya, A. Mathur, S.S. Roy, J.A. McLaughlin, *Diam. & Relat. Mater.* **80**, 59-63 (2017). DOI: <https://doi.org/10.1016/j.diamond.2017.09.001>
- [8] D. Bociaga, A. Sobczyk-Guzenda, W. Szymanski, A. Jedrzejczak, A. Jastrzebska, A. Olejnik, K. Jastrzebski, *Appl. Surf. Sci.* **417**, 23-33 (2017). DOI: <https://doi.org/10.1016/j.apsusc.2017.03.223>
- [9] L. Kolodziejczyk, W. Szymanski, D. Batory, A. Jedrzejczak, *Diam. Relat. Mater.* **67**, 8-15 (2016). DOI: <https://doi.org/10.1016/j.diamond.2015.12.010>
- [10] D. Bociaga, A. Sobczyk-Guzenda, W. Szymanski, A. Jedrzejczak, A. Jastrzebska, A. Olejnik, L. Swiatek, K. Jastrzebski, *Vac.* **143**, 395-406 (2017). DOI: <https://doi.org/10.1016/j.vacuum.2017.06.027>
- [11] L. Huang, J. Yuan, Ch. Li, D. Hong, *Surf. and Coat. Technol.* **353**, 163-170 (2018). DOI: <https://doi.org/10.1016/j.surfcoat.2018.08.076>
- [12] J. Wang, J. Ma, W. Huang, L. Wang, H. He, C. Liu, *Surf. and Coat. Technol.* **316**, 22-29 (2017). DOI: <https://doi.org/10.1016/j.surfcoat.2017.02.065>
- [13] R.D. Mansano, R. Ruas, A.P. Mousinho, L.S. Zambom, T.J.A. Pinto, L.H. Amoedo, M. Massi, *Surf. and Coat. Technol.* **202**, 2813-2816 (2008). DOI: <https://doi.org/10.1016/j.surfcoat.2007.10.012>
- [14] X. Sui, J. Liu, S. Zhang, J. Yang, J. Hao, *Appl. Surf. Sci.* **439**, 24-32 (2018). DOI: <https://doi.org/10.1016/j.apsusc.2017.12.266>
- [15] J. Corona-Gomez, S. Shiri, M. Mohammadtaheri, Q. Yang, *Surf. and Coat. Technol.* **332**, 120-127 (2017). DOI: <https://doi.org/10.1016/j.surfcoat.2017.10.050>
- [16] Z. Ruijun, M. Hongtao, *J. of Mater. Sci.*, **41**, 1705-1709 (2006). DOI: <https://doi.org/10.1115/WTC2005-63323>
- [17] S. Srinivasan, Y. Tang, Y.S.Li, Q. Yang, A. Hirose, *Appl. Surf. Sci.* **258**, 8094-8099 (2012). DOI: <https://doi.org/10.1016/j.apsusc.2012.04.178>
- [18] S. C. Ray, W.F.Pongb, P. Papakonstantinou, *Thin Solid Films* **610**, 42-47 (2016). DOI: <https://doi.org/10.1016/j.tsf.2016.04.048>
- [19] Y. Mabuchi, T. Higuchi, V. Weihnacht, *Tribol. Int.* **62**, 130-140 (2013). DOI: <https://doi.org/10.1016/j.triboint.2013.02.007>
- [20] N. Srinivasana, L. K. Bhaskara, R. Kumara, S. Baragetti, *Mater. and Des.* **160**, 303-312 (2018). DOI: <https://doi.org/10.1016/j.matdes.2018.09.022>
- [21] Y.J. Won, H. Ki, *Appl. Surf. Sci.* **311**, 775-779 (2014). DOI: <https://doi.org/10.1016/j.apsusc.2014.05.161>
- [22] M. Azzi, P. Amirault, M. Paquette, J.E. Klemberg-Sapieha, L. Martinu, *Surf. and Coat. Technol.* **204**, 3986-3994 (2010). DOI: <https://doi.org/10.1016/j.surfcoat.2010.05.004>
- [23] C.F.M. Borges, E. Pfender, J. Heberlein, *Diam. & Relat. Mater.* **10**, 1983-1990 (2001). DOI: [https://doi.org/10.1016/S0925-9635\(01\)00465-4](https://doi.org/10.1016/S0925-9635(01)00465-4)
- [24] M. Azzi, M. Paquette, J.A. Szpunar, J.E. Klemberg-Sapieha, L. Martinu, *Wear* **267**, 860-866 (2009). DOI: <https://doi.org/10.1016/j.wear.2009.02.006>
- [25] M.H. Ghasemi, B. Ghasemi, H.R.M. Semnani, *Diam. & Relat. Mater.* **93**, 8-15 (2019). DOI: <https://doi.org/10.1016/j.diamond.2019.01.016>
- [26] N. Ueda, N. Yamauchi, T. Sone, A. Okamoto, M. Tsujikawa, *Surf. and Coat. Technol.* **201**, 5487-5492 (2007). DOI: <https://doi.org/10.1016/j.surfcoat.2006.07.021>
- [27] Z. Cheng, C.X. Li, H. Dong, T. Bell, *Surf. and Coat. Technol.* **191**, 195-200 (2005). DOI: <https://doi.org/10.1016/j.surfcoat.2004.03.004>
- [28] M. Tsujikawa, N. Yamauchi, N. Ueda, T. Sone, Y. Hirose, *Surf. and Coat. Technol.* **193**, 309-313 (2005). DOI: <https://doi.org/10.1016/j.surfcoat.2004.08.179>
- [29] O. Sharifahmadian, F. Mahboubi, A. Oskouie, *Diam. & Relat. Mater.* **91**, 74-83 (2019). DOI: <https://doi.org/10.1016/j.diamond.2018.11.004>

- [30] O. Sharifahmadian, F. Mahboubi, *Ceram. Int.* **45**, 16424-16432 (2019). DOI: <https://doi.org/10.1016/j.ceramint.2019.05.173>
- [31] O. Sharifahmadian, F. Mahboub, *Ceram. Int.* **45**, 7736-7742 (2019). DOI: <https://doi.org/10.1016/j.ceramint.2019.01.076>
- [32] M. Ebrahimi, F. Mahboubi, M. Reza Naimi-Jamal, *Diam. & Relat. Mater.* **52**, 32-37 (2015).  
DOI: <https://doi.org/10.1016/j.diamond.2014.12.004>
- [33] M. Jokari-Sheshdeha, F. Mahboubi, K. Dehghani, *Diam. & Relat. Mater.* **81**, 77-88 (2018).  
DOI: <https://doi.org/10.1016/j.diamond.2017.11.007>
- [34] C. Tsotsos, A.L. Yerokhin, A.D. Wilson, A. Leyland, A. Matthews, *Wear* **253**, 986-993 (2002).  
DOI: [https://doi.org/10.1016/S0043-1648\(02\)00225-9](https://doi.org/10.1016/S0043-1648(02)00225-9)
- [35] K.H. Lo, C.H. Shek, J.K.L. Lai, *Mater. Sci. and Eng.* **R 65**, 39-104 (2009). DOI: <https://doi.org/10.1016/j.mser.2009.03.001>
- [36] Z. Yu, X. Xu, L. Wang, J. Qiang, Z. Hei, *Surf. and Coat. Technol.* **153**, 125-130 (2002).  
DOI: [https://doi.org/10.1016/S0257-8972\(01\)01670-X](https://doi.org/10.1016/S0257-8972(01)01670-X)
- [37] O. Sharifahmadian, M. Farzad, S. Yazdani, *Diam. & Relat. Mater.* **95**, 60-70 (2019).  
DOI: <https://doi.org/10.1016/j.diamond.2019.04.007>
- [38] M. Tsujikawa, D. Yoshida, N. Yamauchi, N. Ueda, T. Sone, S. Tanaka, *Surf. and Coat. Technol.* **200**, 507-511 (2005).  
DOI: <https://doi.org/10.1016/j.surfcoat.2005.02.051>
- [39] T.L. Christiansen, M.A.J. Somers, *Int. J. Mater. Res.* **100**, 1361-1377 (2009). DOI: <https://doi.org/10.3139/146.110202>
- [40] T. Borowski, K. Kulikowski, B. Adamczyk-Cieślak, K. Roźniatowski, M. Spychalski, M. Tarnowski, *Surf. and Coat. Technol.* **392**, 125705 (2020).  
DOI: <https://doi.org/10.1016/j.surfcoat.2020.125705>